Book Chapter

Optimal Placement and Sizing of Energy Storage System Using Power Sensitivity Analysis in Practical Stand-Alone Microgrid

Dongmin Kim[1], Kipo Yoon[1], Soo Hyoung Lee[2]* and Jung-Wook Park[1]*

[1]School of Electrical & Electronic Engineering, Yonsei University, Korea
[2]Department of Electrical and Control Engineering, Mokpo National University, Korea

***Corresponding Authors:** Soo Hyoung Lee, Department of Electrical and Control Engineering, Mokpo National University, Mokpo 58554, Korea

Jung-Wook Park, School of Electrical & Electronic Engineering, Yonsei University, Seoul 03722, Korea

Published **November 03, 2021**

This Book Chapter is a republication of an article published by Jung-Wook Park, et al. at Electronics in July 2021. (Kim, D.; Yoon, K.; Lee, S.H.; Park, J.-W. Optimal Placement and Sizing of an Energy Storage System Using a Power Sensitivity Analysis in a Practical Stand-Alone Microgrid. Electronics 2021, 10, 1598. https://doi.org/10.3390/electronics10131598)

How to cite this book chapter: Dongmin Kim, Kipo Yoon, Soo Hyoung Lee, Jung-Wook Park. Optimal Placement and Sizing of Energy Storage System Using Power Sensitivity Analysis in Practical Stand-Alone Microgrid. In: Le Nhu Ngoc Thanh, editor. Prime Archives in Electronics. Hyderabad, India: Vide Leaf. 2021.

Author Contributions: This research was conducted with the collaboration of all authors. D.K. and K.Y. wrote the paper; S.H.L. and J.-W.P., supervised the paper. All authors have read and agreed to the published version of the manuscript.

Funding: This work was supported in part by the National Research Foundation of Korea (NRF) (Grant number: 2020R1A3B2079407), the Ministry of Science and ICT (MSIT), Korea and in part by Korea Institute of Energy Technology Evaluation and Planning (KETEP) grant funded by the Korea government (MOTIE) (Grant number: 20192010107050).

Conflicts of Interest: The authors declare no conflict of interest.

Abstract

Energy storage system (ESS) is developing into a very important element to ensure stable operation of the power system. ESS has features of quick control and free charging and discharging. By using these characteristics, it can efficiently respond to sudden events of the power system and is helpful in resolving congested lines caused by excessive output of the distributed generators (DGs) using renewable energy sources (RESs). In order to install new ESSs efficiently and economically in the power system, the following two things must be considered: optimal installation placements and optimal sizes of ESSs. There are many studies on the optimal installation placement and sizing of ESS through analytical approaches, mathematical optimization techniques, and artificial intelligence. This paper presents an algorithm to determine the optimal installation placement and sizing of ESS for virtual multi-slack (VMS) operation based on power sensitivity analysis in the stand-alone microgrid. Through the proposed algorithm, the optimal installation placement could be determined by simple calculation, and the optimal sizing of ESS

for the determined placement could be obtained at the same time. The algorithm is verified through several case studies in the stand-alone microgrid where the practical power system data is reflected.

Keywords

Distribution Network; Energy Storage System; Microgrid; Optimal Placement; Optimal Sizing; Power Sensitivity Analysis; Virtual Multi-Slack Operation

Introduction

Worldwide, the penetration of distributed generators (DGs) using renewable energy sources (RESs) is increasing to solve the environmental pollution problem of conventional fossil fuel generators and high maintenance cost problems due to the aging of the generators. RESs are eco-friendly and sustainable energy sources that do not have pollutants emitted during the power generation process and have no power generation cost by mainly using wind and solar power. However, wind and solar power have intermittent and uncontrollable characteristics, and it is difficult to predict the generations of DGs using them. These disadvantages of DGs using RESs pose new challenges to the stable and reliable operation of the power system in which renewable energy sources are connected at high penetration. It is very difficult to accurately predict the output of RESs such as wind and solar power, and the output fluctuation of DGs using RESs is very large. As a result, the generation-load imbalance of the power system occurs frequently. This uncertainty in DGs using RESs would degrade the stability of the power system and causes frequent frequency fluctuations [1-3]. As the penetration of DGs increases, excessive power generation of it, as well as lack of power generation, causes other stability problems. This excessive power generation of DGs may increase the voltages of specific buses and the congestion of the distribution network, which may cause stability problems in the entire power system.

Recently, energy storage system (ESS) has been developed as an important power system element to solve these stability

problems of the power system caused by increased penetration of DGs [4]. The two most important characteristics of ESS for improving the stability of the power system are as follows: fast charging / discharging features and the ability to store surplus energy. The first contribution of ESS to the stability of the power system is the smoothing of the generation power output by using the fast charging / discharging features. The generation power output of DGs using especially wind and solar power fluctuates very quickly and largely. ESS can mitigate these fluctuations in the generation power output of DGs by rapidly charging in case of an unsuspected increase in the generation power of DGs and discharging in case of a decrease in the generation of DGs. The second contribution of ESS in the power system is the time shifting of the generation power output using the ability to store surplus energy. Unlike in the past, as large-scale DGs are connected to the power system, excessive generation power output of DGs has created new problems such as reverse power flow or increased congestion of lines. When the generation power output of DGs is excessive and it causes a serious mismatch between the power generation-load, the ESS can store part of the excessive generation power output df DGs. Then, the stored energy of ESS could be used when the generation power by the DGs is insufficient or when the load is increased, and as a result, the flexibility of the power system could be secured by using ESS.

In order to connect ESS efficiently and economically to the power system, it is essential to optimize the installation placement and sizing of ESS [5-8]. The technology for ESS has been introduced to increase the stability and economy of power systems resulting from increased penetration of DGs to microgrid, and as a result, optimal localization of ESS is a very important issue to secure the power system stability of microgrid. In addition, since an excessively sized ESS causes high installation costs, many studies on the optimal sizing of ESS are also being conducted. Because there are so many types of power systems including microgrids, and the purpose of installing ESS varies, there is no unique solution for the optimal placement and sizing of newly installed ESS. As a result,

numerous solutions have been studied with the following approaches: analytical approach, mathematical optimization, and artificial intelligence.

In the analytical approach, the optimal placement and sizing of ESS is determined by evaluation according to a set of formulas and algorithms [9-12]. During the optimization process, pre-defined system constraints are repeatedly examined, and the set of parameters containing the optimal placement and sizing of ESS corresponding to the objective function is chosen as the optimal solution. The mathematical optimization approach uses the numerical methods to find the optimal solution [13-17]. As the complexity and dimensions of the power system increase, the computation and time to find the optimal solution may increase exponentially. Finally, unlike analytical approach and mathematical optimization approach, artificial intelligence does not require complex algorithms and computational processes to determine the optimal placement and sizing of ESS [18-20]. While the solutions obtained with artificial intelligence do not guarantee the optimal solution, they could obtain largely satisfactory solutions without complex analysis and mathematical models.

This paper proposes the algorithm for optimal placements and sizes of newly installed ESSs based on power sensitivity analysis as analytical approach. It analyzes all candidate placements within the microgrid where ESS is newly installed. The objective function defined in this paper gives priority to the optimal placement, and the optimal size of the corresponding newly installed ESS could be directly determined by the placement of the installation according to the priority. In this paper, ESS would be operated by virtual multi-slack droop control. As a result, the newly installed ESS could respond with a high contribution to all load changes in the microgrid, while ensuring the voltage stability of the ESS connected bus, and the sizing of the ESS could also be obtained at an appropriate level rather than oversize.

This paper is organized as follows: Section 2 describes VMS operation for the stand-alone microgrid based on power sensitivity analysis. Section 3 shows the algorithm for optimal placement and sizing of newly installed ESS. Thereafter, in Section 4, case studies are carried out on the stand-alone microgrid where the practical power system data is reflected. Finally, the conclusions are given in Section 5.

VMS Power Flow Analysis Based on Power Sensitivity Analysis

There is only one actual slack bus in conventional electric power system, which is to balance the real and reactive power. It is also called to reference bus at the system. The phase angle and voltage magnitude of this actual slack bus are defined on 0° and 1, which are the only fixed elements in the entire power system. Existing power flow analysis is based on this, and in this paper, newly installed ESSs operate as virtual multi-slacks (VMSs) in microgrid. The VMS operations with newly installed ESSs could participate in maintaining the power generation-load balance by helping the actual slack bus. The real and reactive power imbalance in microgrid having total *n* buses are given as:

$$\Delta P_i = P_i - \sum_{j=1}^{n} |V_i||V_j||Y_{ij}|\cos(\theta_{ij} - \delta_i + \delta_j) \quad (1)$$

$$\Delta Q_i = Q_i + \sum_{j=1}^{n} |V_i||V_j||Y_{ij}|\sin(\theta_{ij} - \delta_i + \delta_j) \quad (2)$$

where P_i and Q_i are the scheduled real and reactive power at the *i*-th bus, respectively [20]. And the other term on the right-hand side of (1) and (2) are the actual values of the real and reactive power at the *i*-th bus, respectively. $|V_i|$ and δ_i are the magnitude and phase angle of voltage at the *i*-th bus, respectively. $|Y_{ij}|$ and θ_{ij} are the magnitude and phase angle of the nodal admittance matrix between the *i*-th bus and the *j*-th bus, respectively. By applying the Taylor expansion to (1) and (2) while ignoring the higher-order terms, the linearization

equation for the proposed VMS power flow could be expressed as follows:

$$\begin{bmatrix} \Delta\delta_{ESS} \\ \Delta\delta_{MG} \\ \Delta V_{ESS} \\ \Delta V_{MG} \end{bmatrix} = \begin{bmatrix} \mathrm{J}_{P\delta} & \mathrm{J}_{PV} \\ \mathrm{J}_{Q\delta} & \mathrm{J}_{QV} \end{bmatrix}^{-1} \begin{bmatrix} \Delta P_{ESS} \\ \Delta P_{MG} \\ \Delta Q_{ESS} \\ \Delta Q_{MG} \end{bmatrix}, \quad (3)$$

$$\mathbf{K} = \begin{bmatrix} \mathrm{K}_{11} & \mathrm{K}_{12} \\ \mathrm{K}_{21} & \mathrm{K}_{22} \end{bmatrix} = \begin{bmatrix} \mathrm{J}_{P\delta} & \mathrm{J}_{PV} \\ \mathrm{J}_{Q\delta} & \mathrm{J}_{QV} \end{bmatrix}^{-1}$$

where $\left[\Delta\delta \middle| \Delta V\right]^t$ and $\left[\Delta P \middle| \Delta Q\right]^t$ are the mismatch vectors of voltage and power, respectively. The subscripts, *ESS* and *MG* mean that the values of the ESSs connected buses and the values of the other buses excluding the ESSs connected buses. It is noted that the value for the actual slack bus is not considered. The inverse matrix of Jacobian matrix, **J** ($\in$ ¡ $^{2(n-1)\times 2(n-1)}$) is defined as **K**. Then, the mismatch vector of voltages and powers at the virtual slack buses can be calculated as:

$$\begin{bmatrix} \Delta\delta_{ESS} \\ \Delta\delta_{MG} \\ \Delta V_{ESS} \\ \Delta V_{MG} \end{bmatrix} = \mathbf{K}^{ESS} \begin{bmatrix} \Delta P_{ESS} \\ \Delta Q_{ESS} \end{bmatrix} + \mathbf{K}^{MG} \begin{bmatrix} \Delta P_{ESS} \\ \Delta P_{MG} \\ \Delta Q_{ESS} \\ \Delta Q_{MG} \end{bmatrix} \quad (4)$$

where $\mathbf{K}^{ESS}$ ($\in$ ¡ $^{2(m-1)\times 2(m-1)}$) and $\mathbf{K}^{MG}$ ($\in$ ¡ $^{2(m-1)\times 2(n-1)}$) are reassigned matrices for the virtual slacks (the buses to which newly installed ESSs are connected) and the entire power system as part of **K** in (3). $\mathbf{K}^{ESS}$ includes only the elements of newly installed ESS-connected buses in **K** like as (5). On the other hand, in $\mathbf{K}^{MG}$, all elements of entire buses except only the actual slack bus are covered like as (6).

$$\mathbf{K}^{ESS} = \left[\begin{array}{ccc|ccc} K_{11}(2,2) & \text{L} & K_{11}(2,m) & K_{12}(2,2) & \text{L} & K_{12}(2,m) \\ \text{M} & \text{O} & \text{M} & \text{M} & \text{O} & \text{M} \\ K_{11}(m,2) & \text{L} & K_{11}(m,m) & K_{12}(m,2) & \text{L} & K_{12}(m,m) \\ \hline K_{21}(2,2) & \text{L} & K_{21}(2,m) & K_{22}(2,2) & \text{L} & K_{22}(2,m) \\ \text{M} & \text{O} & \text{M} & \text{M} & \text{O} & \text{M} \\ K_{21}(m,2) & \text{L} & K_{21}(m,m) & K_{22}(m,2) & \text{L} & K_{22}(m,m) \end{array}\right] \tag{5}$$

$$\mathbf{K}^{MG} = \left[\begin{array}{ccc|ccc} K_{11}(2,2) & \text{L} & K_{11}(2,n) & K_{12}(2,2) & \text{L} & K_{12}(2,n) \\ \text{M} & \text{O} & \text{M} & \text{M} & \text{O} & \text{M} \\ K_{11}(m,2) & \text{L} & K_{11}(m,n) & K_{12}(m,2) & \text{L} & K_{12}(m,n) \\ \hline K_{21}(2,2) & \text{L} & K_{21}(2,n) & K_{22}(2,2) & \text{L} & K_{22}(2,n) \\ \text{M} & \text{O} & \text{M} & \text{M} & \text{O} & \text{M} \\ K_{21}(m,2) & \text{L} & K_{21}(m,n) & K_{22}(m,2) & \text{L} & K_{22}(m,n) \end{array}\right] \tag{6}$$

By the general definition of the slack bus, the voltage magnitudes and phase angles of the slack buses including virtual slack buses are ideally specified. From this, it is assumed that there are no mismatches in the voltage magnitude(s) and phase angle(s) of the bus to which the newly installed ESS(s) is(are) connected. As a result, the left-hand side in (4), which represents the mismatch vector of the voltage magnitude and phase angle at the virtual slack buses, is zero in (4), and (4) could be rearranged follows as:

$$\left[\begin{array}{c} \Delta P_{ESS} \\ \Delta Q_{ESS} \end{array}\right] = -\left[\mathbf{K}^{ESS}\right]^{-1} \mathbf{K}^{MG} \left[\begin{array}{c} \Delta P_{ESS} \\ \Delta P_{MG} \\ \Delta Q_{ESS} \\ \Delta Q_{MG} \end{array}\right] = \mathbf{S}^{ESS} \left[\begin{array}{c} \Delta P_{ESS} \\ \Delta P_{MG} \\ \Delta Q_{ESS} \\ \Delta Q_{MG} \end{array}\right] \tag{7}$$

where $\mathbf{S}^{ESS}$ is the power sensitivity matrix between the newly installed ESSs-connected buses and the entire buses. Once calculated power sensitivity matrix, it is possible to determine the power responses of the ESSs, which are operated as virtual slacks, to load changes in the microgrid through a simple calculation.

Proposed Algorithm for Optimal Placement and Sizing of ESS

Using the Jacobian matrix of the stand-alone microgrid, the power sensitivity between the new ESS installation candidate buses and the entire buses would be calculated as shown in (7). Using the calculated power sensitivity matrix, the total power required for the newly installed ESS on the *i*-th bus to respond to all load changes could be calculated as follows:

$$\mathbf{LP}_{ESS,(i,j)} = \mathbf{S}^{ESS,(i,j)}\Delta P_{j+1,Load} + \mathbf{S}^{ESS,(i,n-1+j)}\Delta Q_{j+1,Load} \tag{8}$$

where $\mathbf{LP}_{ESS,(i,j)}$ is the real and reactive power changes of (i+1)-th bus connected ESS at all load changes in the microgrid. $\mathbf{S}^{ESS,(i,j)}$ is the power sensitivity matrix between (i+1)-th bus connected ESS and the entire buses. $\Delta P_{i,Load}$ and $\Delta Q_{i,Load}$ are the real and reactive power changes of i-th bus connected load. The required power for the newly installed ESS on i-th bus to respond to changes in all loads in the microgrid is calculated as follows:

$$SP_{ESS,i} = \sum_{j=1}^{n-1} \mathbf{LP}_{ESS,(i,j)} \tag{9}$$

$$SQ_{ESS,i} = \sum_{j=n}^{2(n-1)} \mathbf{LP}_{ESS,(i,j)} \tag{10}$$

where $SP_{ESS,i}$ and $SQ_{ESS,i}$ are the total contribution of real and reactive power by the newly installed ESS on i-th bus responding to all load changes in the microgrid, respectively. And the required size of the ESS on the i-th bus to respond properly to every individual load change is defined as follows:

$$MP_{ESS,i} = \max(\mathbf{LP}_{ESS,(i,j)})\Big|_{j=1}^{n-1} \tag{11}$$

$$MQ_{ESS,i} = \max(\mathbf{LP}_{ESS,(i,j)})\Big|_{j=n}^{2(n-1)} \tag{12}$$

In this paper, the objective function for the optimal installation placement of ESS is as shown in (13) and the optimal installation placement is determined by priority according to analysis of all candidate placements for the new installation of ESSs.

$$OF_{ESS[k]} = \frac{\sum SP_{ESS,i}}{\sum MP_{ESS,i}} \tag{13}$$

where $OF_{ESS[k]}$ is the objective function for *k*-th placement pair of the newly installed ESS(s). For example, when the number of newly installed ESSs is two and the number of the candidate placement is *m*, there are $m \times (m-1)/2$ pairs for the placements of ESSs.

In this paper, the objective function for the optimal installation placement of ESS is as shown in (13) and the optimal installation placement is determined by priority according to analysis of all candidate placements for the new installation of ESSs. The objective function value could be increased by the higher $SP_{ESS,i}$ and the lower $MP_{ESS,i}$. This means that even low installation costs could be highly involved in all load changes. Figure 1 shows the proposed algorithm for optimal placement and sizing of newly installed ESS based on power sensitivity analysis.

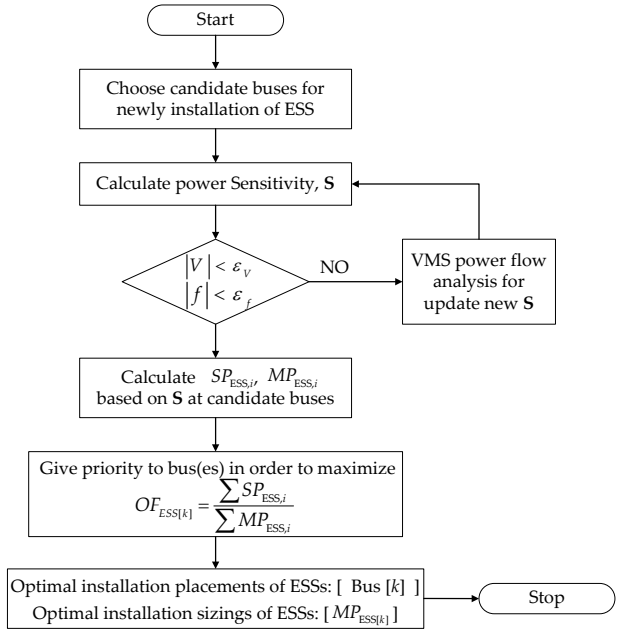

Figure 1: Flowchart for optimal placement and sizing of newly installed ESS based on power sensitivity analysis.

Simulation Results

The proposed algorithm for optimal placement and sizing of newly installed ESS was applied to the stand-alone microgrid in South Korea. This stand-alone microgrid reflects actual power system data and the one-line diagram of the microgrid is shown in Figure 2. It consists of a total of 37 buses, and Bus 1 is an actual slack bus with a diesel generator involved in the stability of the microgrid. The stand-alone microgrid has a total of 21 loads and each load demand is shown in Table 1. Previously, 6 ESSs were connected to the stand-alone microgrid, and 6 ESSs were connected at the following placements: Bus 2, Bus 5, Bus 16, Bus 22, Bus 27, and Bus 31. The actual slack bus and 6 buses with existing ESSs are excluded for the candidate for newly installed ESSs, and there are 30 buses as candidate in the stand-alone microgrid.

It was determined by the proposed algorithm for optimal installation placement and sizing for a newly installed ESS. The voltage stability at the ESS installation placement was verified when all the loads connected to the microgrid were increased sequentially and then decreased. The voltage stability following the optimal sizing of the ESS was compared to the case where the ESS would have been installed at the optimal placement and the case where the ESS would have been installed at the lower priority placement according to the defined objective function.

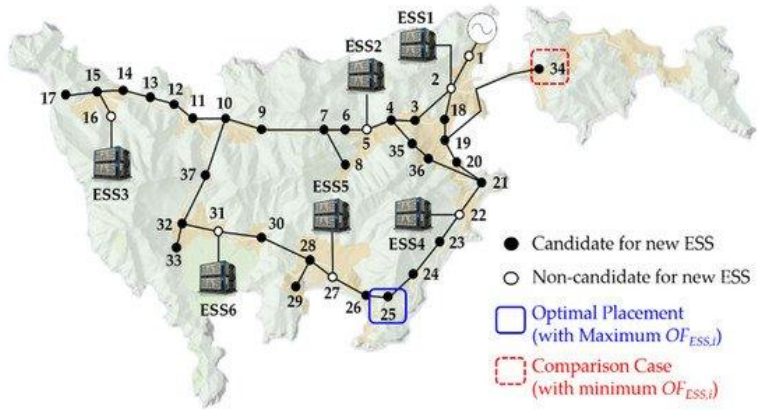

Figure 2: One-line diagram of the stand-alone microgrid in South Korea.

Table 1: Load demands of the stand-alone microgrid.

Bus No.	Load		Bus No.	Load		Bus No.	Load	
	P **(kW)**	***Q*** **(kvar)**		***P*** **(kW)**	***Q*** **(kvar)**		***P*** **(kW)**	***Q*** **(kvar)**
5	92.8	9.28	16	214.4	21.44	27	160	16
7	22.4	2.24	17	323.2	32.32	29	84.16	8.416
8	32	3.2	20	22.4	2.24	30	12.8	1.28
9	38.4	3.84	22	152	15.2	33	28.8	2.88
11	9.6	0.96	23	28.8	2.88	34	101.76	10.176
12	96	9.6	24	41.6	4.16	35	68.8	6.88
14	60.8	6.08	26	41.6	4.16	37	144	14.4

Table 2: Priority analysis according to the installation placement of newly installed an ESS.

Bus No.	$SP_{ESS,i}$ (MW)	$MP_{ESS,i}$ (MW)	$OF_{ESS,i}$	Priority	Recommendation
25	1.125109	0.176325	6.380866	1	High
29	1.040074	0.163066	6.378225	2	High
21	2.031802	0.319182	6.365647	3	High
36	2.038183	0.321272	6.344102	4	High
⋮	⋮	⋮	⋮	⋮	⋮
7	1.842448	0.324621	5.675684	15	Medium
23	1.537929	0.297081	5.176805	16	Medium
33	0.872171	0.168544	5.174735	17	Medium
24	1.424432	0.275621	5.168085	18	Medium
⋮	⋮	⋮	⋮	⋮	⋮
14	1.30429	0.324699	4.016922	27	Low
15	1.277116	0.324909	3.930692	28	Low
17	1.222718	0.3232	3.783163	29	Low
34	1.570997	0.451432	3.48003	30	Low

In order to install new ESS on the microgrid, priorities for all candidate placements are summarized as shown in Table 2 using Figures 1 and (13). A total of 30 candidate buses are prioritized by the defined objective function, with the exception of an actual slack bus and existing 6 ESSs-connected buses. By the defined objective function, Bus 25 is the best placement to install a new ESS and the optimal sizing of the new ESS is 0.176325 MW. On the other hand, Bus 34 is the most inadequate installation placement for a new ESS. The biggest difference between Bus 25 and Bus 34 is that there is no significant difference in $SP_{ESS,i}$ values, but the $MP_{ESS,i}$ value of Bus 34 is remarkably larger than the $MP_{ESS,i}$ value of Bus 25. This means that while there is no significant difference in involvement in responding to changes in all loads, but an excessively high capacity ESS is required in order for Bus 34 to operate in VMS operation for only one specific load change.

Figure 3 shows the voltage stability heatmap for the relationship between all candidate placement for newly installed ESS and all load changes in Table 1. This heatmap clearly and graphically shows the voltage stability between all candidate placements for new ESS and all loads according to power sensitivity matrix through (7). The dark-red and white colors represent the highest sensitivity and zero sensitivity, respectively.

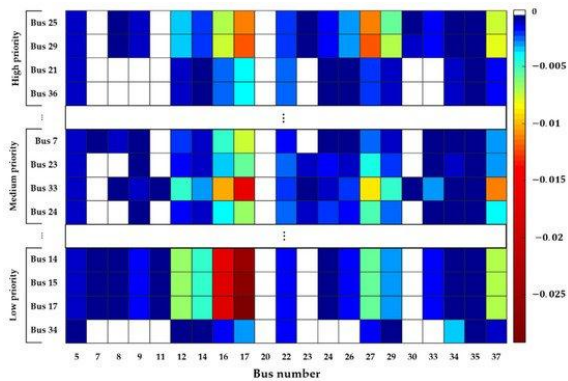

Figure 3: Voltage stability heatmap for the relationship between all candidate placement for ESS and all load changes.

The loads on Bus 16 and Bus 17 are the biggest loads in the microgrid as shown in Table 1. As a result, as shown in Figure 3, changes in the load on Bus 16 and Bus 17 have a significant effect on the voltage stability of all buses. Bus 25 and Bus 29 have a significant impact on the load changes of almost all buses and have relatively small $MP_{ESS,i}$ values as shown in Table 2. On the other hand, Bus 14, Bus 15 and Bus 17 have very high power sensitivity to changes in loads connected to Bus 16 and Bus 17, resulting in high $MP_{ESS,i}$ values. In the case of Bus 34, which has the lowest priority by the proposed algorithm, it has the weakest power sensitivity with other buses, and has the largest $MP_{ESS,i}$ value.

New ESS was installed at the optimal placement (Bus 25) with the optimal sizing, and the VMS operation was verified in sequential changes in all loads. Figure 4 (a) show the real power response of the newly installed ESS, and Figure 4 (b) and (c) show the bus voltage deviation at the installation placement (Bus 25) and the bus voltage deviation at Bus 34. The ESS connected to Bus 25 could respond to all load changes within $MP_{ESS,i}$ obtained by (11), and as a result, the voltage stability of Bus 25 could be improved. Due to the influence of ESS connected to Bus 25, the voltage deviation of Bus 34 was also slightly reduced compared to when ESS was not connected.

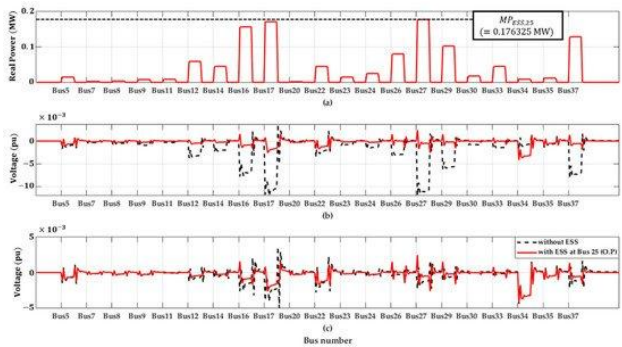

Figure 4: With ESS at optimal placements and sizing, (a) real power respond of ESS, (b) voltage deviation change of Bus 25, and (c) voltage deviation changes of Bus 34 through the VMS operation. O.P, optimal placement

Figure 5 shows the result of VMS operation according to all load changes by connecting new ESS to Bus 34. The sizing of ESS is limited to 0.176325 MW, which is optimal sizing at Bus25 as shown in Figure 5 (a). Unlike Figure 4, when the load on Bus 17 and 34 changes, it could not guarantee that the voltage maintained at normal voltage. This is because the $MP_{ESS,i}$ on Bus 34 is 0.451432 MW as shown in Table 2, but the connected ESS had only 0.176325 MW. As a result, as shown in Figure 5 (c), it is impossible to maintain the voltage due to insufficient capacity of ESS for stable VMS operation respond to load changes on Bus 17 and 34. Furthermore, Figure 5 (b) shows that connecting ESS at Bus 34 could not contribute to improving voltage stability of Bus 25.

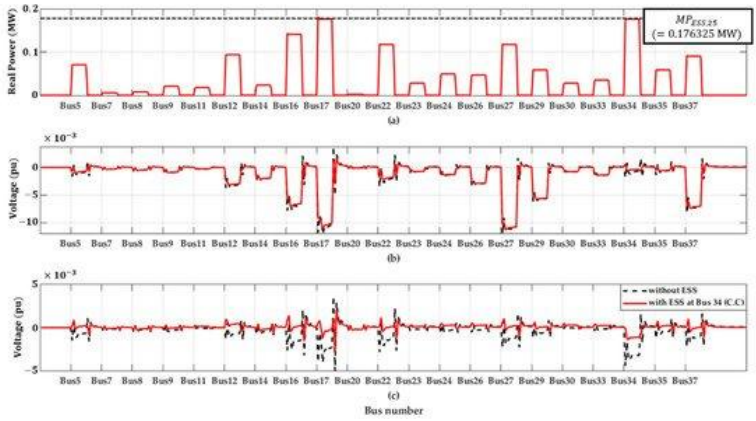

Figure 5: With ESS at Bus 34, (a) real power respond of ESS, (b) voltage deviation change of Bus 25, and (c) voltage deviation change of Bus 34 through the VMS operation. C.C, comparison case.

Figure 6 (a) is the voltage increasing heatmap with improved voltage stability through VMS operation using newly installed ESS with optimal placement (Bus 25) and sizing. That is, when a new ESS is installed to the optimal placement (Bus 25), it shows how much the voltages of each bus, which have decreased by the load changes, are improved compared to the case without ESS (Figure 3). This heatmap shows that the voltage increases with changes in all loads on other buses as well as on the bus (Bus 25) installed new ESS. The dark red

color indicates that the voltage of the case without ESS has increased and the voltage stability is highly increased, and the white color indicates that the voltage stability is similar to that of the case without ESS. As a result, by adding a new ESS to the optimal placement (Bus 25), the voltage stability of not only the bus in which new ESS is installed, but also the other buses in the microgrid is improved. Figure 6 (b) is the voltage increasing heatmap with slightly improved voltage stability by connection of ESS at Bus 34 as comparison case. Compared with Figure 3 and 6 (a), the voltage stability of the entire buses was improved than the case without ESS, but the improvement was less than that of case where new ESS was installed in the optimal placement (Bus 25).

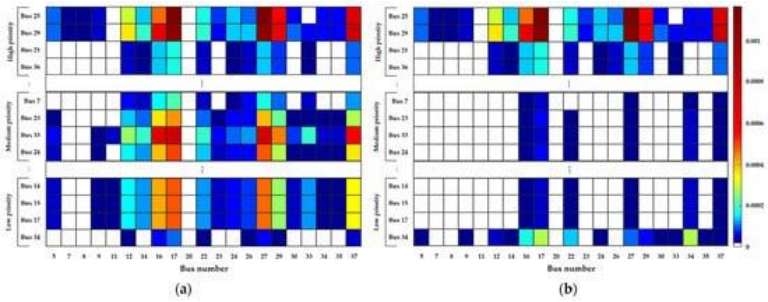

Figure 6: Voltage stability improvement heatmap by (a) new ESS installation at Bus 25 (optimal placement: high recommendation) and (b) new ESS installation at Bus 34 (comparison case: low recommendation) according to the load changes.

Finally, to evaluate the improvement of the voltage stability of the microgrid through VMS operation according to ESS installation and installation placement, root mean square error (*RMSE*) voltage was calculated as follows:

$$\Delta V_{RMSE} = \sqrt{\sum_{l}\sum_{m}\left(\Delta V_{\mathrm{B}(l),\mathrm{L}(m)}\right)^2} \tag{14}$$

where $\Delta V_{\mathrm{B}(i),\mathrm{L}(j)}$ is the voltage variation of *l*-th bus at *m*-th load. The *RMSE* value of the case without ESS is the largest, and the *RMSE* value of the case ESS connected to Bus 25 (optimal placement) is the minimum. This means that when ESS is

installed in the optimal placement, the variation of the entire buses in the microgrid is the smallest in all load changes.

Table 3: Comparison of *RMSE* voltage according to ESS installation and installation placement.

	without ESS	**with ESS at Bus 25 (Optimal placement)**	**with ESS at Bus 34 (Comparison case)**
ΔV_{RMSE}	0.0753	0.0505	0.0731

Conclusions

As the penetration of distributed generators (DGs) using renewable energy sources (RESs) to microgrids increases, the technology of energy storage system (ESS) could play an important role in improving the stability and operational efficiency of the power system. Since the installation cost of ESS is directly related to the installation sizing, it is a very important issue where the optimal placement for the stability of the power system is and how large the optimal sizing is. This paper proposes a novel algorithm for the optimal placement and sizing of newly installed ESS based on power sensitivity analysis and validate it on a practical stand-alone microgrid in South Korea.

The proposed algorithm analyzes all candidates for newly installed ESS in the microgrid based on power sensitivity analysis and determines priorities for optimal installation placements according to the defined objective function. As a result, high-priority placement for newly installed ESS can respond with high involvement to load changes in microgrids with low capacity. An analytic approach method based on power sensitivity analysis allows it to quickly select the optimal placement of the newly installed ESS, and to obtain the optimal sizing of ESS according to the designated installation placement. For all load changes, this paper compares the results of power system operations by newly installed ESS at the optimal placement and by newly installed ESS at the placement with lower priority by the defined objective function. As a result of installing ESS in the optimal placement, the voltage stability of

the bus connected with ESS could be secured. The voltage stability was confirmed by the response of the newly installed ESS to the sequential changes of all loads, and as a result, the appropriateness of the optimal sizing of ESS according to the optimal placement was verified.

References

1. AK Barik, DC Das, A Latif, SMS Hussain, TS Ustun. Optimal Voltage-Frequency Regulation in Distributed Sustainable Energy-Based Hybrid Microgrids with Integrated Resource Planning. Energies. 2021; 14: 2735.
2. B Banerjee, SM Islam. Reliability based optimum location of distributed generation, Int. J. Electr. Power Energy Syst. 2011; 33: 1470–1478.
3. ASA Awad, THM El-Fouly, MMA Salama. Optimal Distributed Generation Allocation and Load Shedding for Improving Distribution System Reliability. Elect. Power Compon. and Syst. 2014; 42.
4. X Tang, K Deng, Q Wu, Y Feng. Optimal Location and Capacity of the Distributed Energy Storage System in a Distribution Network. *IEEE Access*. 2020; 8: 15576-15585.
5. H Xie, X Teng, Y Xu, Y Wang. Optimal Energy Storage Sizing for Networked Microgrids Considering Reliability and Resilience. *IEEE Access*. 2019; 7: 86336-86348.
6. ASA Awad, THM EL-Fouly, MMA Salama. Optimal ESS Allocation for Benefit Maximization in Distribution Networks. *IEEE Trans. Smart Grid*. 2017; 8: 1668-1678.
7. H Yang, SG Choi. Deterministic System Analysis to Guarantee Worst Case Performance for Optimal ESS and PV Sizing. *IEEE Access*. 2019; 7: 98875-98892.
8. LA Wong, VK Ramachandaramurthy SL, Walker, JB Ekanayake. Optimal Placement and Sizing of Battery Energy Storage System Considering the Duck Curve Phenomenon. *IEEE Access*. 2020; 8: 197236-197248.
9. Y Yang, H Li, A Aichhorn, J Zheng, M Greenleaf. Sizing Strategy of Distributed Battery Storage System With High Penetration of Photovoltaic for Voltage Regulation and Peak Load Shaving. *IEEE Trans. Smart Grid*. 2014; 5: 982-991.
10. YM Atwa, EF El-Saadany. Optimal Allocation of ESS in Distribution Systems With a High Penetration of Wind Energy. *IEEE Trans. on Power Syst*. 2010; 25: 1815-1822.

11. A Giannitrapani, S Paoletti, A Vicino, D Zarrilli. Optimal Allocation of Energy Storage Systems for Voltage Control in LV Distribution Networks. IEEE Trans. Smart Grid. 2017; 8: 2859-2870.
12. Y Ru, J Kleissl, S Martinez. Storage Size Determination for Grid-Connected Photovoltaic Systems, IEEE Trans. Sustain. Energy. 2013; 4: 68-81.
13. S Bahramirad, W Reder, A Khodaei. Reliability-Constrained Optimal Sizing of Energy Storage System in a Microgrid. IEEE Trans. Smart Grid. 2012; 3: 2056-2062.
14. I Miranda, N Silva, H Leite. A Holistic Approach to the Integration of Battery Energy Storage Systems in Island Electric Grids With High Wind Penetration. IEEE Trans. Sustain. Energy. 2016; 7: 775-785.
15. H Pandžić, Y Wang, T Qiu, Y Dvorkin, DS Kirschen. Near-Optimal Method for Siting and Sizing of Distributed Storage in a Transmission Network. IEEE Trans. Power Syst. 2015; 30: 2288-2300.
16. SX Chen, HB Gooi, MQ Wang. Sizing of Energy Storage for Microgrids, IEEE Trans. Smart Grid. 2012; 3: 142-151.
17. R Fernández-Blanco, Y Dvorkin, B Xu, Y Wang, DS Kirschen. Optimal Energy Storage Siting and Sizing: A WECC Case Study, IEEE Trans. Sustain. Energy. 2017; 8: 733-743.
18. M Ghofrani, A Arabali, M Etezadi-Amoli, MS Fadali. A Framework for Optimal Placement of Energy Storage Units Within a Power System With High Wind Penetration. IEEE Trans. Sustain. Energy. 2013; 4: 434-442.
19. G Carpinelli, G Celli, S Mocci, F Mottola, F Pilo, et al. Optimal Integration of Distributed Energy Storage Devices in Smart Grids. IEEE Trans. Smart Grid. 2013; 4: 985-995.
20. Karimi Y, Oraee H, Guerrero JM. Decentralized method for load sharing and power management in a hybrid single/three phase-islanded microgrid consisting of hybrid source PV/battery units. IEEE Trans. Power Electron. 2017; 32: 6135–6144.